

Base synergy in freshly nucleated particles

Galib Hasan, Haide Wu, Yosef Knattrup, and Jonas Elm

Department of Chemistry, Aarhus University, Langelandsgade 140, 8000 Aarhus C, Denmark

Correspondence: Jonas Elm (jelm@chem.au.dk)

Abstract. Sulfuric acid (SA), ammonia (AM) and dimethylamine (DMA) are believed to be key contributors to new particle formation (NPF) in the atmosphere. NPF happens through gas-to-particle transformation via cluster formation. However, it is not obvious how small clusters grow to larger sizes and eventually form stable aerosol particles. Recent experimental measurements showed that the presence of mixtures of bases enhance the nucleation rate several orders of magnitude. Using quantum chemistry methods, this study explores this base synergy in the formation of large clusters from a mixture of SA, AM, and DMA. We calculated the binding free energies of the $(SA)_n(AM)_x(DMA)_{n-x}$ clusters, with n from 1 to 10, where x runs from 0 to n . The cluster structures were obtained using our recently developed comprehensive configurational sampling approach based on multiple ABCluster runs and metadynamics sampling via CREST. The structures and thermochemical parameters are calculated at the B97-3c level of theory. The final single point energy of the clusters is calculated at the ω B97X-DJB3/6-311++G(3df,3pd) level of theory.

Based on the calculated thermochemistry, we found that AM, despite being a weaker base, forms more intermolecular interactions than DMA and easily becomes embedded in the cluster core. This leads to the mixed SA-AM/DMA clusters being lower in free energy compared to the pure SA-AM and SA-DMA clusters. We find that the strong base DMA is important in the very initial steps in cluster formation, but for larger clusters an increased ammonia content is found. We also observed that the cluster-to-particle transition point for the mixed SA-AM-DMA clusters occurs at a cluster size of 14 monomers, which is notably smaller than the transition points for the pure SA-AM (16 monomers) or pure SA-DMA (20 monomers) systems. This indicates a strong synergistic effect when both AM and DMA are present, leading to the formation of stable freshly nucleated particles (FNPs) at smaller cluster sizes. These findings emphasize the importance of considering several base molecules, when studying the formation and growth of FNPs.

1 Introduction

Atmospheric aerosols, particularly fine particles ($<1 \mu\text{m}$ in diameter) and ultrafine particles ($<100 \text{ nm}$ in diameter), significantly impact human health by being the primary contributors to air pollution-related mortality (Pelucchi et al., 2009; Cromar K, 2023). Aerosols also directly influence the Earth's energy budget by scattering and absorbing solar radiation, resulting in cooling and warming effects, respectively (Loeb and Kato, 2002). Additionally, they have an even larger indirect effect on the global climate by serving as cloud condensation nuclei (CCN) for the formation of clouds, fog, or mist (Rosenfeld et al., 2014).

To date, the interactions between aerosol particles and clouds remain the least understood process in global climate estimation (Cooley et al., 2023).

Primary aerosols are directly emitted into the atmosphere, while secondary aerosols are formed through gas-to-particle conversion, resulting in the formation of freshly nucleated particles (FNPs). The formation of aerosols is initiated by forming strong hydrogen bonded molecular clusters from different atmospheric vapor molecules (Kulmala et al., 2013). Clusters that possess strong intermolecular interactions can be stable against evaporation, and further grow into aerosol particles of roughly 2 nm and above. Inorganic acids, such as sulfuric acid, and bases, such as ammonia and amines, are key components in the initial cluster formation in the atmosphere (Spracklen et al., 2006; Sipilä et al., 2010; Kirkby et al., 2011; Almeida et al., 2013). In addition, other chemical constituents are also believed to influence clustering such as ions originating from galactic cosmic rays (Kirkby et al., 2016) and condensation of highly oxygenated molecules (HOMs) (Bianchi et al., 2016). To understand the initial stages of atmospheric aerosol formation, it is essential to know the concentrations and chemical composition of the clusters along with the gaseous compounds that contribute to their growth.

Measurements of clusters below 2 nm are extremely challenging, and no comprehensive, simultaneous field measurements of these clusters and their precursors have been conducted until now. Standard condensation particle counters (CPC) typically have detection thresholds around 2-3 nm, making them inadequate for detecting the smallest clusters (McMurry, 2000). While particle size magnifiers (PSM) can detect clusters as small as ~ 1.5 nm, they are expensive, have poor counting efficiency, and do not provide information about the chemical composition of the clusters (Vanhanen et al., 2011). Techniques such as the chemical ionization atmospheric pressure interface mass spectrometer (CI-API-TOF) are necessary to determine the chemical composition of growing clusters (Jokinen et al., 2012). However, these techniques alter the clusters' composition due to fragmentation during the measurement process, leading to potentially inaccurate results (Zapadinsky et al., 2018; Passananti et al., 2019; Alfaouri et al., 2022). The CI-API-TOF can usually only detect clusters up to a certain size of around 10 acid molecules and 10 base molecules (Almeida et al., 2013). This leaves a knowledge gap in the chemical composition of large clusters in the range of 1.0 nm to 2.0 nm. As this is the size range for cluster stabilization, it is crucial to get a better understanding of this unknown cluster-to-particle transition regime (Kulmala et al., 2013). Wu et al. (2023) recently presented a robust computational framework that can be applied to study clustering from single molecules all the way up to 2 nm clusters. Such an approach offers an improved understanding of the chemical interactions and stability of these atmospheric clusters.

Ammonia (AM) and dimethylamine (DMA) are key contributors to the initiation of sulfuric acid (SA) nucleation and greatly enhance the particle formation rates compared to the pure sulfuric acid or sulfuric acid–water systems (Sipilä et al., 2010; Almeida et al., 2013). This happens due to the proton transfer reactions between the acid and base molecules which leads to salt formation. Numerous quantum chemical studies have corroborated the role of bases such as AM (Ianni and Bandy, 1999; Larson et al., 1999; Nadykto and Yu, 2007; Kurtén et al., 2007; Loukonen et al., 2010; Herb et al., 2011; DePalma et al., 2012, 2014) and DMA (Kurtén et al., 2008; Loukonen et al., 2010; Kupiainen-Määttä et al., 2012; Ortega et al., 2012; Olenius et al., 2013b; Nadykto et al., 2014; Henschel et al., 2014; DePalma et al., 2012, 2014; Henschel et al., 2016; Ma et al., 2016) in stabilizing the initial SA clusters.

60 Recent experimental studies have demonstrated that the simultaneous inclusion of both ammonia and amines with sulfuric acid increases new particle formation rates by 10–100 times compared to mixtures containing only sulfuric acid and amines (Glasoe et al., 2015; Yu et al., 2012). This effect cannot be explained by the aqueous-phase base constant or the gas-phase proton affinity, suggesting that the underlying reason for this base synergy is not well understood. One possible explanation is that atmospheric ammonia concentrations are usually much higher than those of amines. However, laboratory experiments
65 demonstrated that when ammonia levels were lower than dimethylamine, the reactions between sulfuric acid and bases still produced nanoparticles with a higher ammonia content compared to dimethylamine (Lawler et al., 2016). This observation suggests that ammonia uptake is driven by a physicochemical effect in the early stages of particle formation, rather than by the relative concentrations of the substances.

Temelso et al. (2018) provided theoretical evidence of base synergy by calculating free energies of three-component molecular clusters composed of sulfuric acid, amine (dimethylamine or trimethylamine), and ammonia. Their findings indicated that adding sulfuric acid to a cluster containing these mixed bases is thermodynamically more favorable than adding it to a cluster with only sulfuric acid and a single type of amine. Myllys et al. (2019) extended the work to larger clusters and provided a molecular-level explanation for the synergistic effects in SA–AM–DMA cluster formation, showing that ammonia can act as a “bridge-former” and is more likely to be protonated than dimethylamine despite having lower gas-phase basicity. Their
75 quantum chemical simulations indicated that ammonia’s inclusion can increase the particle formation rate by up to 5 orders of magnitude compared to the SA–DMA system. However, these studies have been limited to very small clusters of up to eight monomers and thereby does not give insight into the cluster-to-particle transition point of the mixed SA–AM–DMA clusters, nor the AM to DMA ratio in the growing clusters.

Previously, our group has pushed the boundaries of studying large $(SA)_n(AM)_n$ clusters, investigating systems with up
80 to 60 molecules ($n = 30$) to understand the transition from clusters to particles (Engsvang and Elm, 2022; Engsvang et al., 2023). The exponential increase in the number of possible configurations with respect to cluster size required an improved configurational sampling approach as described by Wu et al. (2023). In this work we extended our previous efforts on studying large clusters and perform quantum chemical (QC) calculations on mixed $(SA)_n(AM)_x(DMA)_{n-x}$ clusters, with n from 1 to 10 and $0 \leq x \leq n$. Hence, we study clusters with an acid-to-base ratio of 1:1 and all combinations of AM and DMA for each
85 cluster size. We recently proposed a property-based criteria for defining “freshly nucleated particles (FNPs)”, as the boundary between discrete cluster configurations and bulk particles (Wu et al., 2024). Specifically, we define FNPs as when one or more ions are fully embedded inside the cluster and when the change in the size-averaged binding free energy approaches zero. Hence, the emergence of FNPs acts as the cluster-to-particle transition point. Here we extend this concept to clusters with mixed bases. Our study suggests that mixed clusters possess varying stability, with the introduction of AM becoming
90 increasingly favorable as the cluster size grows, facilitating the cluster-to-particle transition process leading to FNPs at an earlier stage.

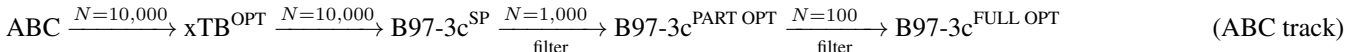
2 Methods

2.1 Computational details

Density functional theory (DFT) calculations during the configurational sampling procedures (single point energies, geometry optimization and vibrational frequency calculations) were performed using the empirically corrected B97-3c method (Brandenburg et al., 2018) in the ORCA 5.0.4 quantum chemistry program (Neese, 2022). Single point energies using ω B97X-D3BJ (Najibi and Goerigk, 2018) with 6-311++G(3df,3dp) (Ditchfield et al., 1971), ma-def2-QZVPP (Zheng et al., 2011), ma-def2-TZVP (Zheng et al., 2011) and def2-TZVDP (Weigend and Ahlrichs, 2005) were also performed in ORCA 5.0.4. The GFN1-xTB (Grimme et al., 2017) and the reparameterized GFN1-xTB^{re-par} based on previous FNP structures (Wu et al., 2024) semi-empirical calculations were performed using the xTB 6.4.0 program (Bannwarth et al., 2021). The reparameterization was performed according to the workflow given by Knattrup et al. (2024) where the energy and gradients of GFN1-xTB were optimized to fit the FNP structures and energies at the B97-3c level of theory. We switched to the GFN1-xTB^{re-par} method once it became available, hence the overall sampling has been performed with a mix of GFN1-xTB and GFN1-xTB^{re-par}. The meta-dynamics calculations were conducted using CREST in non-covalent interaction mode (Pracht et al., 2017, 2020; Pracht and Grimme, 2021; Grimme, 2019; Spicher et al., 2022). Initial clusters were generated with ABCcluster version 3.2 (Zhang and Dolg, 2015, 2016) with a CHARMM force field (Huang and MacKerell Jr, 2013).

2.2 Configurational sampling workflow

We study the (SA)_n(AM)_x(DMA)_{n-x} clusters, with n from 1 to 10 and $0 \leq x \leq n$. This leads to $n + 1$ compositions for each cluster size n , implying that we have to sample many of the largest (SA)₇₋₁₀(base)₇₋₁₀ cluster structures. We employed our recently established configurational sampling protocol, presented by Wu et al. (2023, 2024), demonstrating an excellent balance between accuracy and computational cost. The configurational sampling procedure can be outlined as follows:



Initial cluster structures were generated through 10 parallel ABCcluster runs, yielding a total of 10,000 local minima configurations. Our previous studies (Wu et al., 2023, 2024) confirmed that conducting multiple parallel ABCcluster explorations provides more accurate predictions for the global energy minimum structures of large clusters compared to a single, prolonged exploration. We used ionic monomers but maintained the overall cluster charge neutral, to facilitate proton transfer, as this is typically observed in the lowest free energy clusters. Subsequent geometry optimizations were performed on all these clusters using the GFN1-xTB semi-empirical method (Grimme et al., 2017). DFT single-point calculations were then conducted using the B97-3c method (Brandenburg et al., 2018) on top of the GFN1-xTB optimized conformers.

Next, we filtered out high energy configurations by selecting only the 1,000 lowest structures for partial optimization at the B97-3c level. This partial optimization step was chosen to save computational time and eliminate energetically high-lying configurations. From these, we chose the 100 lowest energy configurations for full optimization and vibrational frequency calculations.

The lowest free energy conformer was then selected for CREST exploration as suggest by Knattrup et al. (2024), which
125 involves metadynamics to provide reasonably good geometries using the following workflow:

CREST $\xrightarrow{N=100}$ B97-3c^{FULL OPT} (CREST track)

The CREST exploration was performed using GFN1-xTB/GFN1-xTB^{re-par} in non-covalent interaction mode. We selected the
100 best geometries from the CREST optimization and performed full optimizations and quasi-harmonic vibrational frequency
calculations (Grimme, 2012) to obtain the corresponding Gibbs free energies. The overall workflow is highly computationally
130 demanding, but should yield a good estimate of the lowest free energy structures.

2.3 Cluster Binding Free Energies

We calculated the cluster standard binding free energies by subtracting the free energy of the cluster to the sum of the free
energies of the individual monomers. It is calculated as follows:

$$\Delta G_{\text{bind}} = G_{\text{cluster}} - \sum_i G_{\text{monomer},i} \quad (1)$$

135 In a similar manner the electronic binding energies and the binding thermal correction to the free energy can be calculated.
This allows the division of the binding free energy in the following terms:

$$\Delta G_{\text{bind}} = \Delta E_{\text{bind}} + \Delta G_{\text{bind, thermal}} \quad (2)$$

Here we calculated the structures and thermochemistry at the B97-3c level (the $\Delta G_{\text{bind, thermal}}$ term) and the binding electronic
energy at the ω B97X-DJB3/6-311++G(3df,3pd) level (the ΔE_{bind} term). We refer to benchmark calculations in the supporting
140 information for a justification of applying the ω B97X-DJB3/6-311++G(3df,3pd) level for single point energies. It should be
noted that the $\Delta G_{\text{bind, thermal}}$ term is calculated using the quasi-harmonic approximation (Grimme, 2012) as default in ORCA.
The quasi-harmonic approximation removes spurious low vibrational modes, but does not take local and global anharmonicity
into account. The recent work by Halonen (2024) provides a promising avenue to further improve our understanding of cluster
stability, by deriving an analytical expression to account for local anharmonicity. Integrating this approach in future studies
145 would increase the accuracy of our thermodynamic predictions, but as it is not straight forward how to obtain the energy
barriers between cluster configuration, it is beyond the scope of the current work.

The equations above account solely for the thermochemistry of the clusters. To calculate the “actual” binding free energies
under specific conditions, we use the self-consistent distribution function (Wilemski and Wyslouzil, 1995; Halonen, 2022):

$$\Delta G_{\text{bind}}(\mathbf{p}) = \Delta G_{\text{bind}} - RT \cdot \left(1 - \frac{1}{n}\right) \cdot \sum_i \ln \left(\frac{p_i}{p_{\text{ref}}}\right) \quad (3)$$

150 Here p_{ref} corresponds to a reference pressure (1 atm) and p_i represents monomer partial pressures. The self-consistent for-
mulation allow us to correctly establish the monomer free energies as zero. We previously (Wu et al., 2024) tested various
formulations of the actual free energies at given conditions and found no deviations between the calculated free energies.

2.4 Size-averaged Binding Free Energies

155 From the standard binding free energies, we also calculate the size averaged binding free energies ($\Delta G_{\text{bind}}/m$) of the clusters. The physical interpretation of this quantity can be seen by analyzing $\Delta G_{\text{bind}}/m$ as a function of cluster size. As the cluster size increases a convergence in the $\Delta G_{\text{bind}}/m$ will be seen toward the formation free energy of the bulk system (Sindel et al., 2022). The physical significance of $\Delta G_{\text{bind}}/m$ can be realized by considering the difference in average binding free energy between a very large (SA)₉₉(base)₉₉ cluster and a (SA)₁₀₀(base)₁₀₀ cluster. The addition of one extra acid-base pair would
160 have little impact on the total free energy of the cluster and thereby the gradient of $\Delta G_{\text{bind}}/m$ becomes zero, resembling the bulk particle phase.

2.5 The convex hull approach

The emergence of fully coordinated ions in a cluster yield information on the transition from discrete cluster configurations to
165 wards the particle phase. In a small cluster all monomers are fully exposed to the exterior and a large stabilization in free energy is gained, when adding more monomers to the cluster. In larger cluster structures fully coordinated ions emerge, corresponding to a “solvated” ion with a solvation shell. Adding more monomers to the existing solvation shell leads to less stabilization free energy gained compared to a smaller cluster.

To investigate when the first fully coordinated ion appears in our calculated cluster structures we here applied the 3-
170 dimensional convex hull approach as described by Wu et al. (2024). The applied algorithm is freely available at:
<https://gitlab.com/AndreasBuchgraitz/clusteranalysis>

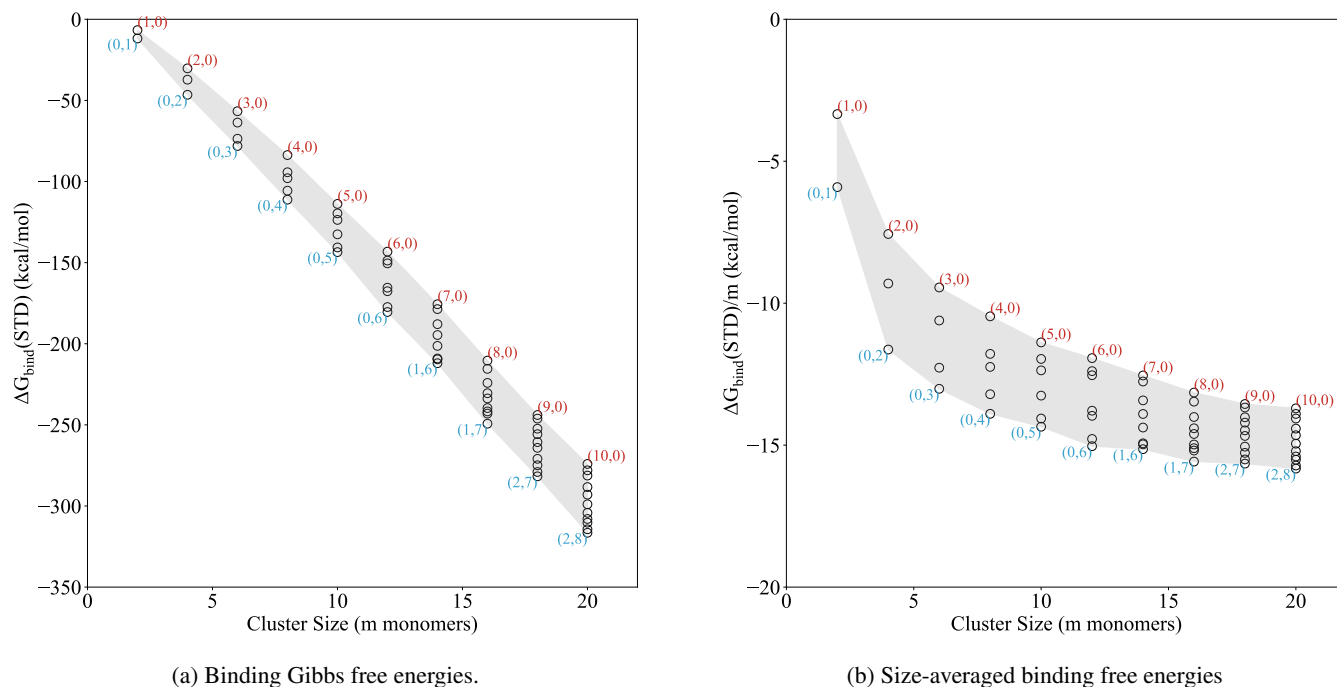
2.6 Cluster-to-particle transition point

Section 2.4 and 2.5 both yield inferred evidence to the transition from clusters to particles. Using the 3D-convex hull approach
175 we can identify when the first solvation shell is formed in the clusters. Structurally, this implies that we are transitioning from a cluster towards a particle. Thermodynamically, when the size-averaged ($\Delta G_{\text{bind}}/m$) as a function of cluster size becomes constant (the gradient of the change of $\Delta G_{\text{bind}}/m$ approaches zero), the cluster behaves more like the bulk than a cluster. Hence, we define the cluster-to-particle transition point as when both these conditions are satisfied. I.e. structurally there must be the development of a new phase by having at least one fully coordinated ion and the thermochemistry must resemble the
180 bulk by leveling out in the $\Delta G_{\text{bind}}/m$ as a function of cluster size. Putting a strict number to when the change in $\Delta G_{\text{bind}}/m$ resembles the bulk is tricky and most likely system dependent. Hence, tentatively we assign roughly a change of $\sim 1 \text{ kcal mol}^{-1}$ in the $\Delta G_{\text{bind}}/m$ from cluster size m to $m + 1$ as the convergence point.

3 Results and discussion

3.1 Binding Free Energy at Standard Condition

185 Applying the outlined extensive cluster sampling approach we studied the mixed $(SA)_n(AM)_x(DMA)_{n-x}$ clusters, with n from 1 to 10 and $0 \leq x \leq n$. The pure SA–AM and SA–DMA clusters are taken from Wu et al. (2024), with refined ω B97X-D3BJ/6-311++G(3df,3pd) single point energies calculated in this work. Figure 1a presents the standard binding free energies, calculated at 298.15 K and 1 atm, as a function of the number of monomers m in the cluster. Each point on the graph is labeled with a pair (AM, DMA), indicating the numbers of ammonia and dimethylamine monomers in the cluster.



190

Figure 1. (a) Binding Gibbs free energy and (b) size-averaged binding Gibbs free energy of the $(SA)_n(AM)_x(DMA)_{n-x}$ clusters, with n from 1 to 10 and $0 \leq x \leq n$, under standard condition (298.15 k and 1 atm). The free energies are calculated at the ω B97X-D3BJ/6-311++G(3df,3pd)//B97-3c level of theory.

Based on the standard binding free energies (Figure 1a), we see that the SA–DMA clusters are the most stable up to 12 monomers. Beyond this point, it is more favorable to exchange 1-2 DMA molecules with AM. Comparing the AM to DMA ratio for smaller clusters, the (5,0) cluster is significantly higher in free energy, by almost 20 kcal/mol, compared to the (0,5) cluster, indicating that DMA alone provides substantial stability for the small cluster sizes.

195 For cluster sizes around 14–16 monomers, compositions only containing SA and DMA are correspondingly 2.9 kcal/mol and 9.4 kcal/mol higher in free energies than (1,6) and (1,7), suggesting that introducing one AM molecule increases the stability compared to only having DMA in the clusters. This trend is also observed for larger clusters, where the clusters with

compositions only containing SA and DMA are higher in free energies compared to (2,7) and (2,8), indicating that having one or two AM molecules in addition to DMA provides higher stability for the larger clusters.

200 Figure 1b presents the size averaged binding free energies ($\Delta G_{\text{bind}}/m$). These values represent the average binding free energy of each molecule in the cluster. Similar to our previous work (Engsvang and Elm, 2022; Engsvang et al., 2023; Wu et al., 2023, 2024) we see that the size-averaged free energy rapidly decrease as a function of cluster size and levels out around 12–20 monomers. This can be interpreted as the cluster transitioning towards more particle-like properties.

Using the convex hull method from Wu et al. (2024), we studied the formation of solvation shells for clusters with the lowest 205 free energy at each size. When the cluster is composed only of SA and DMA (6,0), no encapsulation of ions occurs. However, when AM is added, the lowest free energy structure favors a shell structure, with AM encapsulated by SA and DMA in clusters of size (1,6) to (1,7) (see Figure 2a). When two AM molecules are introduced, a single solvation shell forms, encapsulating both AM monomers as shown in Figure 2b.

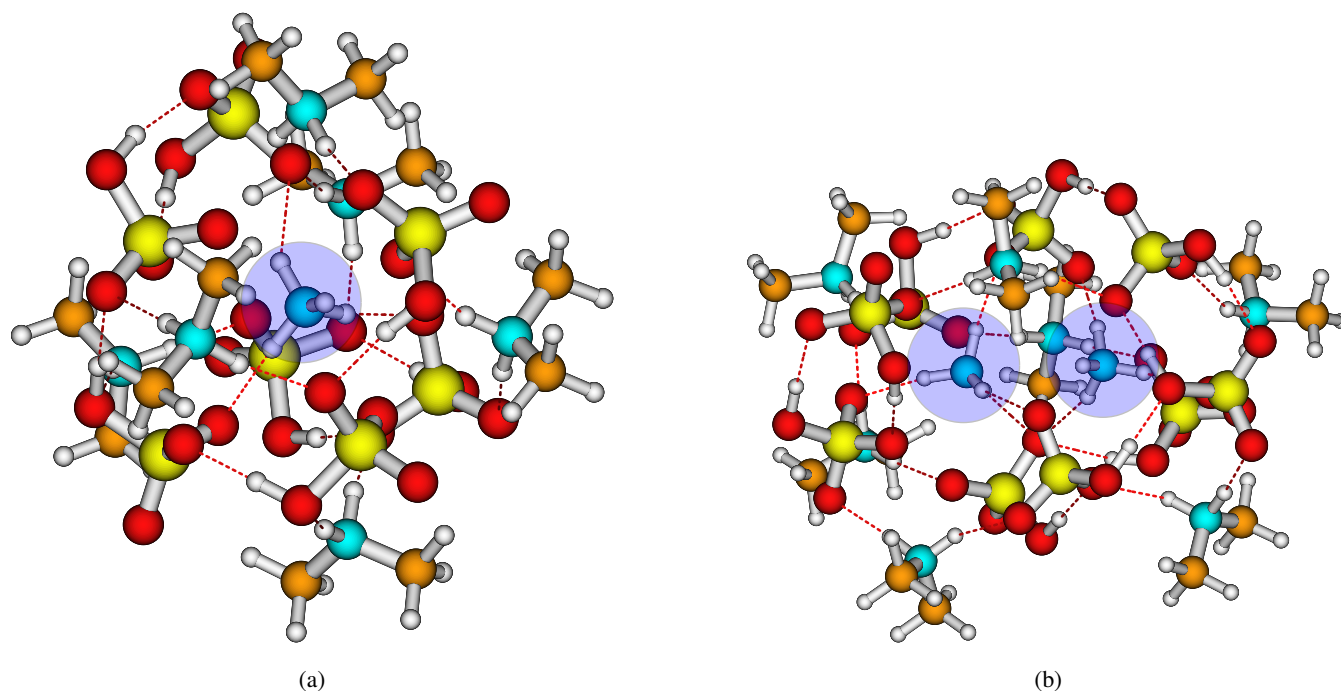


Figure 2. Two examples of protonated ammonia (blue circle) being encapsulated for (a) $(\text{SA})_7(\text{AM})_1(\text{DMA})_6$, (b) $(\text{SA})_9(\text{AM})_2(\text{DMA})_7$. The structures are the lowest in free energy at the $\omega\text{B97X-D3BJ/6-311++G(3df,3pd)//B97-3c}$ level of theory. White = hydrogen, blue = nitrogen, yellow = sulfur, red = oxygen, and brown = carbon.

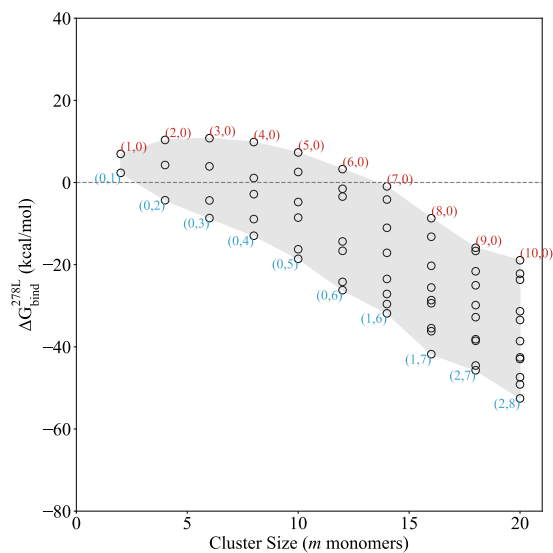
210 The reason for the more stable clusters containing 1-2 AM molecules can be ascribed to an intricate combination of hydrogen bond capacity, base strength and steric hindrance. For instance, the T_d symmetry of the AM molecule makes it capable of forming four intermolecular bonds, whereas DMA can only form two intermolecular bonds. This will become increasingly important as the cluster becomes larger and thus more spherical, as it increases the possible coordination. In addition, the

presence of the two bulky methyl groups in DMA impose a strong steric hindrance. As a result, the protonated AM stays
215 embedded at the center of the cluster and forms a fully coordinated complex with the surrounding HSO_4^- ions. This trend
suggests that AM starts to play a more significant role in stabilizing larger clusters, and its presence becomes increasingly
favorable as the cluster size grows. This is consistent with the experimental work by Lawler et al. (2016) that found increased
AM content compared to DMA in newly formed SA–AM–DMA nanoparticles. A consequence of these findings is that the
cluster-to-particle transition point differs significantly in the mixed base clusters compared to the pure SA–AM and SA–DMA
220 clusters. Hence, the cluster-to-particle transition point occurs at a cluster size of 14 monomers for SA–AM–DMA, compared
to 16 for the SA–AM system and 20 for the SA–DMA system. These FNP sizes are based on that we see the first emergence of
a fully coordinated ion and the leveling out in the size-averaged free energies (see definition in section 2.6). In addition, these
cluster-to-particle transition points corresponds to 15.0 Å, 16.7 Å and 17.3 Å for the SA–AM–DMA, SA–AM and SA–DMA
systems, respectively. We note that the cluster-to-particle transition point identified from our previous work (Wu et al., 2024)
225 was unchanged by the single point refinement. Overall, this implies that there is a synergistic effect between the bases AM and
DMA for the formation of freshly nucleated particles (FNPs).

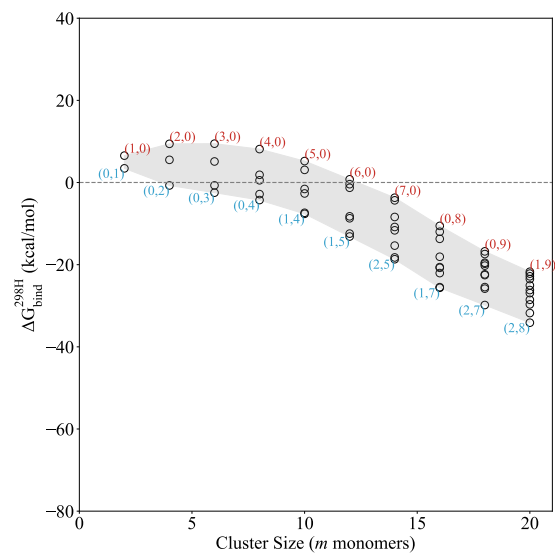
3.2 Binding Free Energies at Given Conditions

Based on the calculated binding Gibbs free energies at standard conditions described in previous section, we can evaluate the
binding free energies under certain monomer concentration and temperature conditions using equation (3). Figure 3 presents
230 the binding free energies of the clusters at 278.15 K and 298.15 K. We considered two specific conditions: a low concen-
tration regime ($[\text{SA}] = 10^7$ molecules cm^{-3} , $[\text{DMA}] = 1$ ppt, $[\text{AM}] = 10$ ppt) and a high concentration regime ($[\text{SA}] =$
 10^7 molecules cm^{-3} , $[\text{DMA}] = 10$ ppt, $[\text{AM}] = 10$ ppb). These concentrations and temperatures align with typical condi-
tions employed in the CLOUD chamber experiments (Almeida et al., 2013; Kürten et al., 2018) and real-world nucleation
observations (Kürten et al., 2014). To better relate our findings to real atmospheric environments, our studied temperature and
235 concentration regimes can be linked to conditions observed in real atmosphere. For instance, in line with previous studies
conducted in Hyytiälä, Finland, which represent typical boreal forest environments, we considered sulfuric acid (SA) concen-
trations and temperatures that are relevant for new particle formation (NPF) processes. In these environments, SA concen-
trations are often in the range of $[\text{SA}] = 10^4$ – 10^8 molecules cm^{-3} , with temperatures that generally range between 278.15 K and
298.15 K, depending on seasonal variations. These temperature and concentration conditions closely resemble the boundary
240 layer conditions that are frequently encountered in temperate regions (Jokinen et al., 2021).

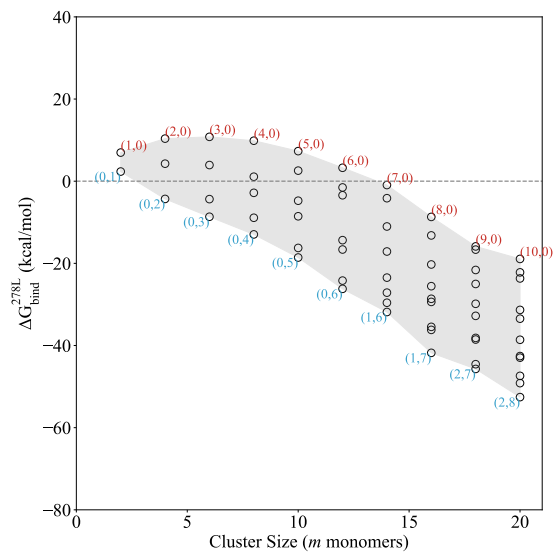
However, we do note that for clean environments the “low conc.” regime applied here, might still represent an upper bound.
We also tested the effect of decreasing $[\text{SA}]$ to 10^6 molecules cm^{-3} or increasing to 10^8 molecules cm^{-3} (See Figures S1-S3
in the SI). In the following, we will go through each scenario.



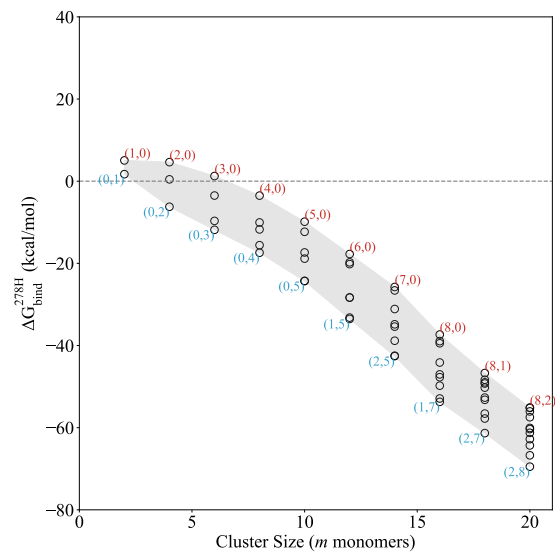
(a) 298.15 K - Low conc.



(b) 298.15 K - High conc.



(c) 278.15 K - Low conc.



(d) 278.15 K - High conc.

245

Figure 3. Binding Gibbs free energy, at the ω B97X-D3BJ/6-311++G(3df,3pd)//B97-3c level of theory of the $(SA)_n(AM)_x(DMA)_{n-x}$ clusters, with $n = x$ between 1 and 10, at given condition of temperature (298.15 K and 278.15 K) and different monomer concentration. Monomer concentrations of [SA] was fixed at 10^7 molecules cm^{-3} . “High conc.” refers to [AM] = 10 ppb, [MA] = [DMA] = 10 ppt. “Low conc.” refers to [AM] = 10 ppt, [MA] = [DMA] = 1 ppt.

Low concentrations, 298.15 K

Similar to the standard free energies in previous section, the actual free energies in Figure 3a, show that the clusters have lower free energy when they are composed of 1–2 AM molecules for the larger cluster sizes. This scenario is seen from the smallest composition with 14 monomers to the largest cluster composition with 20 monomers. However, the clusters do predominantly contain DMA compared to AM. Across all the studied cluster sizes the clusters with a high AM content are generally higher in binding free energies compared to those with a mix of AM and DMA or higher DMA content. We see that the pure SA–AM clusters have a nucleation barrier with a critical cluster at 6 monomers. This is not the case when the clusters are composed of only SA–DMA and is less pronounced for the SA–AM–DMA clusters with mixed bases. These finding aligns with the experimental results of Glasoe et al. (2015), which demonstrated that the formation of 1.8 nm sulfuric acid–base particles followed the trend: AM < MA < DMA < TMA , where MA is methylamine and TMA is trimethylamine.

At low base concentration, changing the SA concentration has a major influence on the results (See SI). At $[SA] = 10^6$ molecules cm^{-3} there is a nucleation barrier in all systems and particles are unlikely to form. At $[SA] = 10^8$ molecules cm^{-3} the critical cluster is reduced to 4 monomers.

High concentrations, 298.15 K

In Figure 3b, we see a much narrower span in the binding free energies at given conditions compared to Figure 3a. This is primarily caused by an increased stability of the SA–AM clusters due to higher concentration of AM. On the contrary the SA–DMA clusters are much less affected by the increased concentration as they already have relatively low evaporation rates. The binding free energies are generally more negative compared to the low concentration regime at 298.15 K, logically indicating greater stability at higher concentrations. These results are consistent with the previous work by Olenius et al. (2013a), Besel et al. (2020) and Kubecka et al. (2023). Due to the high concentration of AM = 10 ppb, we see AM molecules emerging in the lowest free energy clusters at much smaller sizes such as in (1,4) and (1,5). In a similar manner two AM molecules are also found in the cluster at smaller sizes of (2,5).

Similar to the low concentration scenario, lowering the SA concentration to 10^6 molecules cm^{-3} leads to higher free energies (See SI). Interesting, this also leads to the emergence of three AM molecules in the $m = 16$ cluster. Increasing the SA concentration to 10^8 molecules cm^{-3} does not change the trends of the system.

Low concentrations, at 278.15 K

Looking at the binding free energies at 278.15 K and low concentration (Figure 3c), the clusters with 1–2 ammonia are again lowest in free energies at larger sizes. This scenario is observed across all cluster compositions. Clusters such as (1,6–7) and (2,7–8) show the lowest binding free energies, indicating that the clusters are more stable with a higher proportion of DMA. Hence, the composition of the lowest free energy clusters are consistent with the 298.15 K and low concentration systems shown in Figure 3a. This could indicate that the concentration and not the temperature is primary driver in determining the

lowest free energy cluster compositions. We see a small nucleation barrier in the SA–AM system with a critical cluster of 6 monomers, but no barrier in the other systems.

280 Changing the SA concentration does not change the trends at 278.15 K and low base concentration (See SI).

High concentrations, at 278.15 K

Figure 3d shows similar trends as the situation at 298.15 K and high concentrations (Figure 3b). Hence, the the lowest free energy composition is the same as at the higher temperature. Obviously, the clusters are lower in free energy compared to the higher temperature. There is seen no nucleation barriers in any of the studied systems with the free energy surface being
285 downhill. Again at low temperature, changing the SA concentration does not change the trends (See SI).

Overall, our results reveal that at low concentrations, the inclusion of DMA in the clusters tends to yield lower, more negative, binding free energies. In contrast, clusters with a higher proportion of AM alone are less stable in the low concentration regime and more stable in high concentration regime. These findings underscore the importance of DMA in the initial “*cluster stabilization*” regime, but also shows the importance of ammonia in facilitating the cluster-to-particle transition, leading to the
290 onset of FNPs in the “*freshly nucleated particle (FNP)*” regime. These results align with the previous hypothesis by Elm et al. (2017); Elm (2017, 2020) that suggested that strong bases like DMA or diamines play a crucial role in the very initial stages of cluster formation, while the subsequent growth is driven by weaker bases such as AM.

4 Conclusions

Here we studied the formation of large clusters composed of sulfuric acid (SA), ammonia (AM) and dimethylamine (DMA).
295 Using quantum chemical methods we studied the mixed $(SA)_n(AM)_x(DMA)_{n-x}$ cluster systems, with n from 1 to 10 and $0 \leq x \leq n$ at the ω B97X-D3BJ/6-311++G(3df,3pd)//B97-3c level of theory. We found that the pure SA–DMA clusters are the most stable up to a cluster size of around 8–12 monomers, depending on precursor concentrations, without the need for AM. As the cluster size increases beyond 10–14 monomers, adding 1–3 ammonia molecules significantly increases the stability of the cluster. This suggests a synergistic effect where the presence of a small number of ammonia molecules, in addition to DMA,
300 enhances the overall stability of the sulfuric acid clusters, especially at larger cluster sizes. Additionally, in most of the clusters, AM molecules are embedded in the core, making strong intermolecular interactions with SA, while the DMA molecules reside on the periphery of the cluster. Moreover, we found that the cluster-to-particle transition point in the mixed SA–AM–DMA system occurs at a smaller cluster size of 14 monomers, in contrast to 16 monomers for SA-AM and 20 monomers for SA–DMA found in the previous study by Wu et al. (2024). This suggests a significant synergistic effect when both AM and DMA
305 are present, resulting in the formation of freshly nucleated particles (FNPs) at smaller cluster sizes. The identified base synergy between AM and DMA indicates that nucleation mechanisms are inherently complex and further work is require to study the synergistic effects between other vapours. Hence, additional vapours such as methyl amine (MA) and methane sulfonic acid (MSA) could be interesting to study in the future, as well as the growth of FNPs via uptake of SA, bases and organics.

Code availability. The code used to compute the solvation shells using the convex hull algorithm is available at:
310 <https://gitlab.com/AndreasBuchgraitz/clusteranalysis>

Data availability. All the calculated structures and thermochemistry are available in the Atmospheric Cluster Database (ACDB) (Elm, 2019)

Author contributions. Conceptualization: J.E.;
Methodology: G.H., H. W., Y.K., J.E.;
Formal analysis: G.H., H. W., Y.K.;
315 Investigation: G.H., H. W., Y.K.;
Resources: J.E.;
Writing - original draft: G.H., H. W., Y.K., J.E.;
Writing - review & editing: G.H., H. W., Y.K., J.E.;
Visualization: G.H., H. W., Y.K.;
320 Project administration: J.E.;
Funding acquisition: J.E.;
Supervision: J.E.

Competing interests. At least one of the (co-)authors is a member of the editorial board of Aerosol Research. The authors have no other competing interests to declare.

325 *Acknowledgements.* Funded by the European Union (ERC, ExploreFNP, project 101040353). Views and opinions expressed are however those of the authors only and do not necessarily reflect those of the European Union or the European Research Council Executive Agency. Neither the European Union nor the granting authority can be held responsible for them.

This work was funded by the Danish National Research Foundation (DNRF172) through the Center of Excellence for Chemistry of Clouds.

330 The numerical results presented in this work were obtained at the Centre for Scientific Computing, Aarhus <https://phys.au.dk/forskning/faciliteter/cscaa/>.

References

- Alfaouri, D., Passananti, M., Zanca, T., Ahonen, L., Kangasluoma, J., Kubečka, J., Myllys, N., and Vehkamäki, H.: A Study on the Fragmentation of Sulfuric Acid and Dimethylamine Clusters Inside an Atmospheric Pressure Interface Time-of-flight Mass Spectrometer, *Atmos. Meas. Tech.*, 15, 11–19, 2022.
- Almeida, J., Schobesberger, S., Kürten, A., Ortega, I. K., Kupiainen-Määttä, O., Praplan, A. P., Adamov, A., Amorim, A., Bianchi, F., Breitenlechner, M., and et al.: Molecular Understanding of Sulphuric Acid-Amine Particle Nucleation in the Atmosphere, *Nature*, 502, 359–363, 2013.
- Bannwarth, C., Caldeweyher, E., Ehlert, S., Hansen, A., Pracht, P., Seibert, J., Spicher, S., and Grimme, S.: Extended tight-binding quantum chemistry methods, *WIREs Computational Molecular Science*, 11, e1493, <https://doi.org/https://doi.org/10.1002/wcms.1493>, 2021.
- Besel, V., Kubečka, J., Kürten, T., and Vehkamäki, H.: Impact of quantum chemistry parameter choices and cluster distribution model settings on modeled atmospheric particle formation rates, *The Journal of Physical Chemistry A*, 124, 5931–5943, 2020.
- Bianchi, F., Tröstl, J., Junninen, H., Frege, C., Henne, S., Hoyle, C. R., Molteni, U., Herrmann, E., Adamov, A., Bukowiecki, N., et al.: New particle formation in the free troposphere: A question of chemistry and timing, *Science*, 352, 1109–1112, 2016.
- Brandenburg, J. G., Bannwarth, C., Hansen, A., and Grimme, S.: B97-3c: A revised low-cost variant of the B97-D density functional method, *The Journal of Chemical Physics*, 148, 064 104, <https://doi.org/10.1063/1.5012601>, 2018.
- Cooley, S., Schoeman, D., Bopp, L., Boyd, P., Donner, S., Kiessling, W., Martinetto, P., Ojea, E., Racault, M., Rost, B., et al.: Oceans and coastal ecosystems and their services, 2023.
- Cromar K, L. N.: Risk communication of ambient air pollution in the WHO European Region: review of air quality indexes and lessons learned., 2023.
- DePalma, J. W., Bzdek, B. R., Doren, D. J., and Johnston, M. V.: Structure and Energetics of Nanometer Size Clusters of Sulfuric Acid with Ammonia and Dimethylamine, *J. Phys. Chem. A*, 116, 1030–1040, 2012.
- DePalma, J. W., Doren, D. J., and Johnston, M. V.: Formation and Growth of Molecular Clusters Containing Sulfuric Acid, Water, Ammonia, and Dimethylamine, *J. Phys. Chem. A*, 118, 5464–5473, 2014.
- Ditchfield, R., Hehre, W. J., and Pople, J. A.: Self-Consistent Molecular-Orbital Methods. IX. An Extended Gaussian-Type Basis for Molecular-Orbital Studies of Organic Molecules, *J. Chem. Phys.*, 54, 724–728, <https://doi.org/10.1063/1.1674902>, 1971.
- Elm, J.: Elucidating the limiting steps in sulfuric acid–base new particle formation, *The Journal of Physical Chemistry A*, 121, 8288–8295, 2017.
- Elm, J.: An Atmospheric Cluster Database Consisting of Sulfuric Acid, Bases, Organics, and Water, *ACS Omega*, 4, 10 965–10 974, 2019.
- Elm, J.: Toward a holistic understanding of the formation and growth of atmospheric molecular clusters: a quantum machine learning perspective, *The Journal of Physical Chemistry A*, 125, 895–902, 2020.
- Elm, J., Passananti, M., Kurtén, T., and Vehkamäki, H.: Diamines can initiate new particle formation in the atmosphere, *The Journal of Physical Chemistry A*, 121, 6155–6164, 2017.
- Engsvang, M. and Elm, J.: Modeling the Binding Free Energy of Large Atmospheric Sulfuric Acid–Ammonia Clusters, *ACS omega*, 7, 8077–8083, 2022.
- Engsvang, M., Kubečka, J., and Elm, J.: Toward Modeling the Growth of Large Atmospheric Sulfuric Acid–Ammonia Clusters, *ACS omega*, 8, 34 597–34 609, 2023.

- Glase, W., Volz, K., Panta, B., Freshour, N., Bachman, R., Hanson, D., McMurry, P., and Jen, C.: Sulfuric acid nucleation: An experimental study of the effect of seven bases, *Journal of Geophysical Research: Atmospheres*, 120, 1933–1950, 2015.
- 370 Grimme, S.: Supramolecular Binding Thermodynamics by Dispersion-corrected Density Functional Theory, *Chem. Eur. J.*, 18, 9955–9964, 2012.
- Grimme, S.: Exploration of chemical compound, conformer, and reaction space with meta-dynamics simulations based on tight-binding quantum chemical calculations, *Journal of chemical theory and computation*, 15, 2847–2862, 2019.
- Grimme, S., Bannwarth, C., and Shushkov, P.: A robust and accurate tight-binding quantum chemical method for structures, vibrational 375 frequencies, and noncovalent interactions of large molecular systems parametrized for all spd-block elements ($Z= 1-86$), *Journal of chemical theory and computation*, 13, 1989–2009, 2017.
- Halonen, R.: A consistent formation free energy definition for multicomponent clusters in quantum thermochemistry, *Journal of Aerosol Science*, 162, 105 974, 2022.
- Halonen, R.: Assessment of Anharmonicities in Clusters: Developing and Validating a Minimum-Information Partition Function, *Journal of 380 Chemical Theory and Computation*, 2024.
- Henschel, H., Navarro, J. C. A., Yli-Juuti, T., Kupiainen-Määttä, O., Olenius, T., Ortega, I. K., Clegg, S. L., Kurtén, T., Riipinen, I., and Vehkamäki, H.: Hydration of atmospherically relevant molecular clusters: Computational chemistry and classical thermodynamics, *J. Phys. Chem. A.*, 118, 2599–2611, 2014.
- Henschel, H., Kurtén, T., and Vehkamäki, H.: Computational study on the effect of hydration on new particle formation in the sulfuric 385 acid/ammonia and sulfuric acid/ dimethylamine systems, *J. Phys. Chem. A.*, 120, 1886–1896, 2016.
- Herb, J., Nadykto, A. B., and Yu, F.: Large Ternary Hydrogen-bonded Pre-nucleation Clusters in the Earth’s Atmosphere, *Chem. Phys. Lett.*, 518, 7–14, 2011.
- Huang, J. and MacKerell Jr, A. D.: CHARMM36 all-atom additive protein force field: Validation based on comparison to NMR data, *Journal of computational chemistry*, 34, 2135–2145, 2013.
- 390 Ianni, J. C. and Bandy, A. R.: A Density Functional Theory Study of the Hydrates of $\text{NH}_3 \cdot \text{H}_2\text{SO}_4$ and its Implications for the Formation of New Atmospheric Particles, *J. Phys. Chem. A.*, 103, 2801–2811, 1999.
- Jokinen, T., Sipilä, M., Junninen, H., Ehn, M., Lönn, G., Hakala, J., Petäjä, T., Mauldin Iii, R., Kulmala, M., and Worsnop, D.: Atmospheric sulphuric acid and neutral cluster measurements using CI-API-TOF, *Atmospheric Chemistry and Physics*, 12, 4117–4125, 2012.
- Jokinen, T., Lehtipalo, K., Thakur, R. C., Ylivinkka, I., Neitola, K., Sarnela, N., Laitinen, T., Kulmala, M., Petäjä, T., and Sipilä, M.: 395 Measurement report: Long-term measurements of aerosol precursor concentrations in the Finnish sub-Arctic boreal forest, *Atmospheric Chemistry and Physics Discussions*, 2021, 1–22, 2021.
- Kirkby, J., Curtius, J., Almeida, J., Dunne, E., Duplissy, J., Ehrhart, S., Franchin, A., Gagne, S., Ickes, L., Kürten, A., et al.: Role of Sulphuric Acid, Ammonia and Galactic Cosmic Rays in Atmospheric Aerosol Nucleation, *Nature*, 476, 429 – 433, 2011.
- Kirkby, J., Duplissy, J., Sengupta, K., Frege, C., Gordon, H., Williamson, C., Heinritzi, M., Simon, M., Yan, C., Almeida, J., et al.: Ion- 400 induced nucleation of pure biogenic particles, *Nature*, 533, 521–526, 2016.
- Knattrup, Y., Kubečka, J., Wu, H., Jensen, F., and Elm, J.: Reparameterization of GFN1-xTB for Atmospheric Molecular Clusters: Applications to Multi-Acid–Multi-Base Systems, *RSC Adv.*, 14, 20 048–20 055, <https://doi.org/10.1039/D4RA03021D>, 2024.
- Kubecka, J., Neefjes, I., Besel, V., Qiao, F., Xie, H.-B., and Elm, J.: Atmospheric sulfuric acid–multi-base new particle formation revealed through quantum chemistry enhanced by machine learning, *The Journal of Physical Chemistry A*, 127, 2091–2103, 2023.

- 405 Kulmala, M., Kontkanen, J., Junninen, H., Lehtipalo, K., Manninen, H. E., Nieminen, T., Petäjä, T., Sipilä, M., Schobesberger, S., Rantala, P., et al.: Direct observations of atmospheric aerosol nucleation, *Science*, 339, 943–946, 2013.
- Kupiainen-Määttä, O., Ortega, I. K., Kurtén, T., and Vehkamäki, H.: Amine substitution into sulfuric acid - ammonia clusters, *Atmos. Chem. Phys.*, 12, 3591–3599, 2012.
- Kürten, A., Jokinen, T., Simon, M., Sipilä, M., Sarnela, N., Junninen, H., Adamov, A., Almeida, J., Amorim, A., Bianchi, F., et al.: Neutral molecular cluster formation of sulfuric acid–dimethylamine observed in real time under atmospheric conditions, *Proceedings of the National Academy of Sciences*, 111, 15 019–15 024, 2014.
- 410 Kürten, A., Li, C., Bianchi, F., Curtius, J., Dias, A., Donahue, N. M., Duplissy, J., Flagan, R. C., Hakala, J., Jokinen, T., et al.: New particle formation in the sulfuric acid–dimethylamine–water system: reevaluation of CLOUD chamber measurements and comparison to an aerosol nucleation and growth model, *Atmospheric Chemistry and Physics*, 18, 845–863, 2018.
- 415 Kurtén, T., Torpo, L., Sundberg, M. R., Kerminen, V., Vehkamäki, H., and Kulmala, M.: Estimating the $\text{NH}_3\text{:H}_2\text{SO}_4$ Ratio of Nucleating Clusters in Atmospheric Conditions using Quantum Chemical Methods, *Atmos. Chem. Phys.*, 7, 2765–2773, 2007.
- Kurtén, T., Loukonen, V., Vehkamäki, H., and Kulmala, M.: Amines are Likely to Enhance Neutral and Ion-induced Sulfuric Acid-water Nucleation in the Atmosphere More Effectively than Ammonia, *Atmos. Chem. Phys.*, 8, 4095–4103, 2008.
- Larson, L. J., Largent, A., and Tao, M.: Structure of the Sulfuric Acid – Ammonia System and the Effect of Water Molecules in the Gas
420 Phase, *J. Phys. Chem. A.*, 103, 6786–6792, 1999.
- Lawler, M. J., Winkler, P. M., Kim, J., Ahlm, L., Tröstl, J., Praplan, A. P., Schobesberger, S., Kürten, A., Kirkby, J., Bianchi, F., et al.: Unexpectedly acidic nanoparticles formed in dimethylamine–ammonia–sulfuric-acid nucleation experiments at CLOUD, *Atmospheric chemistry and physics*, 16, 13 601–13 618, 2016.
- Loeb, N. G. and Kato, S.: Top-of-atmosphere direct radiative effect of aerosols over the tropical oceans from the Clouds and the Earth’s
425 Radiant Energy System (CERES) satellite instrument, *Journal of Climate*, 15, 1474–1484, 2002.
- Loukonen, V., Kurtén, T., Ortega, I. K., Vehkamäki, H., Pádua, A. A. H., Sellegri, K., and Kulmala, M.: Enhancing Effect of Dimethylamine in Sulfuric Acid Nucleation in the Presence of Water - A Computational Study, *Atmos. Chem. Phys.*, 10, 4961–4974, 2010.
- Ma, Y., Chen, J., Jiang, S., Liu, Y., Huang, T., Miao, S., Wang, C., and Huang, W.: Characterization of the nucleation precursor ($\text{H}_2\text{SO}_4\text{-(CH}_3)_2\text{NH}$) complex: Intra-cluster interactions and atmospheric relevance, *RSC Adv.*, 6, 5824–5836, 2016.
- 430 McMurtry, P. H.: The history of condensation nucleus counters, *Aerosol Science & Technology*, 33, 297–322, 2000.
- Myllys, N., Chee, S., Olenius, T., Lawler, M., and Smith, J.: Molecular-level understanding of synergistic effects in sulfuric acid–amine–ammonia mixed clusters, *The Journal of Physical Chemistry A*, 123, 2420–2425, 2019.
- Nadykto, A. B. and Yu, F.: Strong Hydrogen Bonding between Atmospheric Nucleation Precursors and Common Organics, *Chem. Phys. Lett.*, 435, 14–18, 2007.
- 435 Nadykto, A. B., Herb, J., Yu, F., and Xu, Y.: Enhancement in the production of nucleating clusters due to dimethylamine and large uncertainties in the thermochemistry of amine-enhanced nucleation, *Chem. Phys. Lett.*, 609, 42–49, 2014.
- Najibi, A. and Goerigk, L.: The Nonlocal Kernel in van der Waals Density Functionals as an Additive Correction: An Extensive Analysis with Special Emphasis on the B97M-V and ω B97M-V Approaches, *J. Chem. Theory Comput.*, 14, 5725–5738, <https://doi.org/10.1021/acs.jctc.8b00842>, 2018.
- 440 Neese, F.: Software update: The ORCA program system—Version 5.0, *WIREs Comput. Mol. Sci.*, 12, e1606, 2022.
- Olenius, T., Kupiainen-Määttä, O., Ortega, I., Kurtén, T., and Vehkamäki, H.: Free energy barrier in the growth of sulfuric acid–ammonia and sulfuric acid–dimethylamine clusters, *The Journal of chemical physics*, 139, 2013a.

- Olenius, T., Kupiainen-Määttä, O., Ortega, I. K., Kurtén, T., and Vehkamäki, H.: Free energy barrier in the growth of sulfuric acid-ammonia and sulfuric acid-dimethylamine clusters, *J. Chem. Phys.*, 139, 084312, 2013b.
- 445 Ortega, I. K., Kupiainen-Määttä, O., Kurtén, T., Olenius, T., Wilkman, O., McGrath, M. J., Loukonen, V., and Vehkamäki, H.: From quantum chemical formation free energies to evaporation rates, *Atmos. Chem. Phys.*, 12, 225–235, 2012.
- Passananti, M., Zapadinsky, E., Zanca, T., Kangasluoma, J., Myllys, N., Rissanen, M. P., Kurtén, T., Ehn, M., Attoui, M., and Vehkamäki, H.: How well can we predict cluster fragmentation inside a mass spectrometer?, *Chemical Communications*, 55, 5946–5949, 2019.
- Pelucchi, C., Negri, E., Gallus, S., Boffetta, P., Tramacere, I., and La Vecchia, C.: Long-term Particulate Matter Exposure and Mortality: A
450 Review of European Epidemiological Studies, *BMC Public Health*, 9, 453, 2009.
- Pracht, P. and Grimme, S.: Calculation of absolute molecular entropies and heat capacities made simple, *Chemical science*, 12, 6551–6568, 2021.
- Pracht, P., Bauer, C. A., and Grimme, S.: Automated and efficient quantum chemical determination and energetic ranking of molecular protonation sites, *Journal of Computational Chemistry*, 38, 2618–2631, 2017.
- 455 Pracht, P., Bohle, F., and Grimme, S.: Automated exploration of the low-energy chemical space with fast quantum chemical methods, *Physical Chemistry Chemical Physics*, 22, 7169–7192, 2020.
- Rosenfeld, D., Andreae, M. O., Asmi, A., Chin, M., de Leeuw, G., Donovan, D. P., Kahn, R., Kinne, S., Kivekäs, N., Kulmala, M., et al.: Global observations of aerosol-cloud-precipitation-climate interactions, *Reviews of Geophysics*, 52, 750–808, 2014.
- Sindel, J. P., Gobrecht, D., Helling, C., and Decin, L.: Revisiting Fundamental Properties of TiO₂ Nanoclusters as Condensation Seeds in
460 Astrophysical Environments, *Astron. Astrophys.*, 668, A35, <https://doi.org/10.1051/0004-6361/202243306>, 2022.
- Sipilä, M., Berndt, T., Petäjä, T., Brus, D., Vanhanen, J., Stratmann, F., Patokoski, J., Mauldin III, R. L., Hyvärinen, A.-P., Lihavainen, H., et al.: The role of sulfuric acid in atmospheric nucleation, *Science*, 327, 1243–1246, 2010.
- Spicher, S., Plett, C., Pracht, P., Hansen, A., and Grimme, S.: Automated molecular cluster growing for explicit solvation by efficient force field and tight binding methods, *Journal of Chemical Theory and Computation*, 18, 3174–3189, 2022.
- 465 Spracklen, D., Carslaw, K., Kulmala, M., Kerminen, V.-M., Mann, G., and Sihto, S.-L.: The contribution of boundary layer nucleation events to total particle concentrations on regional and global scales, *Atmospheric Chemistry and Physics*, 6, 5631–5648, 2006.
- Temelso, B., Morrison, E. F., Speer, D. L., Cao, B. C., Appiah-Padi, N., Kim, G., and Shields, G. C.: Effect of mixing ammonia and alkylamines on sulfate aerosol formation, *The Journal of Physical Chemistry A*, 122, 1612–1622, 2018.
- Vanhanen, J., Mikkilä, J., Lehtipalo, K., Sipilä, M., Manninen, H., Siivola, E., Petäjä, T., and Kulmala, M.: Particle size magnifier for
470 nano-CN detection, *Aerosol Science and Technology*, 45, 533–542, 2011.
- Weigend, F. and Ahlrichs, R.: Balanced Basis Sets of Split Valence, Triple Zeta Valence and Quadruple Zeta Valence Quality for H to Rn: Design and Assessment of Accuracy, *Phys. Chem. Chem. Phys.*, 7, 3297–3305, <https://doi.org/10.1039/B508541A>, 2005.
- Wilemski, G. and Wyslouzil, B. E.: Binary nucleation kinetics. I. Self-consistent size distribution, *The Journal of chemical physics*, 103, 1127–1136, 1995.
- 475 Wu, H., Engsvang, M., Knattrup, Y., Kubecka, J., and Elm, J.: Improved Configurational Sampling Protocol for Large Atmospheric Molecular Clusters, *ACS omega*, 8, 45065–45077, 2023.
- Wu, H., Knattrup, Y., Jensen, A. B., and Elm, J.: Cluster-to-particle transition in atmospheric nanoclusters, *Aerosol Research Discussions*, 2024, 1–20, 2024.
- Yu, H., McGraw, R., and Lee, S.-H.: Effects of amines on formation of sub-3 nm particles and their subsequent growth, *Geophysical Research
480 Letters*, 39, 2012.

- Zapadinsky, E., Passananti, M., Myllys, N., Kurte'n, T., and Vehkama`ki, H.: Modeling on fragmentation of clusters inside a mass spectrometer, *The Journal of Physical Chemistry A*, 123, 611–624, 2018.
- Zhang, J. and Dolg, M.: ABCluster: the artificial bee colony algorithm for cluster global optimization, *Phys. Chem. Chem. Phys.*, 17, 24 173–24 181, <https://doi.org/10.1039/C5CP04060D>, 2015.
- 485 Zhang, J. and Dolg, M.: Global optimization of clusters of rigid molecules using the artificial bee colony algorithm, *Phys. Chem. Chem. Phys.*, 18, 3003–3010, <https://doi.org/10.1039/C5CP06313B>, 2016.
- Zheng, J., Xu, X., and Truhlar, D. G.: Minimally augmented Karlsruhe basis sets, *Theor. Chem. Acc.*, 128, 295–305, <https://doi.org/10.1007/s00214-010-0846-z>, 2011.